Water and acrylamide monomer transfer rates from a settling basin to groundwaters

Stéphane Binet, Kathy Bru, Thomas Klinka, Solène Touzé, Mikael Motelica-Heino

Water and acrylamide monomer transfer rates from a settling basin to groundwaters

Stéphane Binet [1,2], Kathy Bru[3], Thomas Klinka[3], Solène Touzé [3] , Mickael Motelica-Heino [2]

[1] Université de Toulouse ; INP, UPS; CNRS ; EcoLab (Laboratoire Ecologie Fonctionnelle et Environnement); ENSAT, Avenue de l'Agrobiopole, 31326 Castanet Tolosan, France

[2] Université d'Orléans ; CNRS ; UMR7327 ; INSU ; Institut des Sciences de la Terre d'Orléans (ISTO) Bureau de Recherches Géologiques et Minières (BRGM)

[3] Bureau de Recherches Géologiques et Minières (BRGM), BP. 36009, 45060 Orléans Cedex 2, France

Corresponding author: stephane.binet@univ-orleans.fr

Abstract:

The aim of this paper was to estimate the potential leakage of acrylamide monomer, used for flocculation in a settling basin, towards the groundwaters. Surface-groundwater interactions were conceptualized with a groundwater transport model, using a transfer rate to describe the clogged properties of the interface. The change in the transfer rate as a function of the spreading of the clogged layer in the settling basin was characterized with respect to time. It is shown that the water and the Acrylamide transfer rate are not controlled by the spreading of the clogged layer until this layer fully covers the interface. When the clogged layer spreads out, the transfer rate remains in the same order of magnitude until the area covered reaches 80%. The main flux takes place through bank seepage. In these early stage conditions of a working settling basin, the acrylamide flux towards groundwaters remains constant, at close to 10 g/yr (± 5).

Key word: Acrylamide; Water transfer rate; Clogged layer; Groundwater

1. Introduction:

Emerging contaminants are compounds that were previously not detectable but that are now being found in groundwater. The environmental routes by which these compounds enter groundwaters, their toxicity and the potential risks to drinking water and aquatic ecosystems are a source of great concern (Stuart et al. 2012). One of these contaminants is acrylamide (AMD), a carcinogenic, mutagenic and reprotoxic monomer (Stuart et al. 2012). AMD is a process residue associated to the use of polyacrylamide (PAM)-based flocculants. These flocculants are used by quarries to improve the separation of suspended particles in water and hence its clarification and recycling in the treatment plant. All the papers dealing with AMD in natural waters report the presence of AMD in significant concentrations after PAM-based flocculants were used (Brown & Rhead 1979; Chu & Metcalfe 2007; Croll et al. 1974). Recent progress in AMD measurements shows the presence of AMD in the surface waters and sediment pore waters of the settling basins used in an aggregates quarry (Touzé et al. 2014). The relationship between quarry basin and the surrounding groundwater quality has already been well demonstrated (Muellegger et al. 2013).

A number of studies have been conducted to estimate the biodegradation of AMD in the environment. Results generally indicate that there is a widespread microbial ability to degrade AMD in various environments, soils, sediments and water (Guezennec et al. 2014). However, the reactivity of AMD in low concentration conditions such as groundwater has rarely been studied. So far, no significant reactivity has been demonstrated in groundwaters and no significant adsorption was observed in sediment composed of 90% sand and 10% feldspar (Mnif, et al. 2014).

The second key parameter to estimate the mass flux toward the groundwater is the water transfer rate (Sophocleous et al., 2002). Based on Darcy's law the water flux (Qi [m^3/day]) through this interface with a surface (A [m^2]) is described using a transfer rate (ϕ [1/day]) and the head difference (Δh [meter]) between the basin and the groundwaters (Eq. 1).

$Qi = A \phi \Delta h$ (Eq. 1)

In many hydrological contexts, the transfer rate between surface water and groundwater changes with time related to an increase in the infiltration rate (Binet et al. 2007), or related to the cover change in the interface properties (Binet et al. 2006). In settling basins, low permeability sediments create a clogged layer at the interface between surface and ground water. This clogged layer can be a pollution retention zone (Dechesne et al. 2004) or an interface. It is an unconsolidated layer, with time dependent properties (Siriwardene et al. 2007). This interface spreads out, increases in thickness and changes the hydraulic properties of the interface. Schubert (2002) reports that the transfer rate of clogged areas varies with the dynamic hydrology and cannot be regarded as a constant. The transfer rate of the riverbed is therefore a major factor determining the volume of bank filtrate, and may evolve in space and in time (Rosenberry & Pitlick, 2009) from high values controlled by the aquifer hydraulic conductivity to a low value controlled by the low hydraulic conductivity and thickness of the clogged layers. Clogging of inflow regions produces heterogeneous subsurface clay deposits even when the bed is initially homogeneous (Packman & Mackay 2003). Kalbus et al. (2009) observed that a homogeneous low-K streambed, a case often implemented in regional-scale groundwater flow models, resulted in a strong homogenization of fluxes, which may have important implications for the estimation of peak mass flows. All these papers highlight that fluxes are controlled by the interface heterogeneities.

The aim of this article is to determine the mass flux of AMD seeping from a settling basin toward the groundwaters. Knowing the behavior of AMD in porous media and applying the hydrology concepts of lake / groundwater interactions (Sophocleous, 2002), the annual mass flux can be estimated. To achieve this, a groundwater transport model was developed. Calibration of the model is based on pumping and tracer test field scale experiments, coupled with a mapping of the interface clogging. The mass flux of AMD was estimated from the AMD concentration in surface water and the properties of the clogged layer, assuming conservative conditions of AMD in groundwater. The

hypotheses are confronted with field observations of water heads and AMD in groundwater. The discussion focuses on the reactivity of AMD in the aquifers and on the relationship between the water transfer rate and the spread of the clogged layer in the basin.

2. Methods for the characterization of surface water/ groundwater interactions

2.1. Case study: geometric characterization and hydraulic heads

The settling basins are located in an alluvial plain, 1.5 km from the river. The studied basin is used for the storage of the fine particles contained in the process water of an aggregates treatment plant (Touzé et al. 2014). Figure 1 shows the study area. The black rectangle delineates the modeled zone. Limits of the model were defined to be parallel to the observed groundwater flow. The settling basin is divided into two sub-basins, B1 and B2, where the water head fluctuations were recorded using an OTT® probe. In 2010, construction of the embankment between B1 and B2 had not been finished but this was completed by the 2011-2013 monitoring period. Basin B1 has been in use since September 2011. Its surface is about 19 030m² and the average water flow rate entering the basin is 500 m^3/day. The flow rate of fines is estimated to be about 6,700 t (dry weight)/year. Basin B2 is unexploited. Five observation wells were drilled around these basins. PZ1, PZ2 and PZ3 were used for water head monitoring with a mini OTT® probe. PZB and PZC are about 10 m apart. They were used for pumping and tracer tests.

Elevations above sea level of the water head observation points were measured using a Differential GPS method with an accuracy of about 10 cm (Solution G.N.S.S., 2007). The regional water flow is from south-east to north-west, according to the water table map, and was measured in February 2012.

2.2. Characterization of water transfer rate and properties of the clogged layer

The thickness and spatial distribution of the settling sediment deposits in basin B1 were mapped using bathymetric methods and differential GPS (Bru, 2014). First the bottom of the basin was

mapped in May 2011 i.e. before commissioning. The elevation of the bottom bed was recalculated using the water table observed on the day of the experiment. The dataset was interpolated using the kriging method to create a digital elevation model (DEM) of the basin bottom. Mapping was then performed 3 times, in November 2011, June 2012 and October 2012. The difference between the three DEMs gave the thickness and the extent of the settling sediments that clogged the interface between surface water and groundwater. From this a volume of clogged sediments and an error range on the volume induced by the method were calculated.

The water transfer rate (ϕ) [1/day] was deduced from the water balance of the basin. The inputs of the system are the amount of water [m^3/day] from the quarry process (Q_{ex}) and the precipitation waters (Q_{rain}). The outputs are the infiltrated water (Qi) and the evapotranspirated water (Q_{ETR}). Thus, the water balance of the basin can be expressed as follows:

$$\Delta Q_S = Q_{Rain} + Q_{ex} - Qi - Q_{ETR} \qquad \text{(Eq. 2)}$$

where ΔQ_S is the change in the water stored in the basin.

During the closure days of the quarry, Q_{ex}=0, and if the discharge (Qi) is expressed as a function of the basin surface (S_I [m^2]):

$$Qi = (RR + \Delta S - ETR) * S_I \qquad \text{(Eq. 3)}$$

where RR is the precipitation [meter/day)], ΔS the water table change [meter/day] and ETR the evapotranspiration [meter/day)]. The values of RR and ETP were recorded by the French meteorological network. The weather station is located 13 km from the study basin.

The head difference (Δh) [m] between the basin and the aquifer was estimated using the PZ1 observation well:

$$\Delta h = h_{B1} - h_{PZ1} \qquad \text{(Eq. 4)}$$

Thus, the observed transfer rate (ϕ_o [1/day]) can be estimated:

$$\emptyset o = \frac{Qi}{S_l \Delta h} \qquad \text{(Eq. 5)}$$

2.3. Evaluation of groundwater migration using a transport model

One solution to estimate the mass flux towards the groundwater is to apply a conceptual model of surface water /groundwater interactions (Binet et al. 2013), but this approach does not enable the spatial variability of these interactions and the change in time of the hydraulic properties to be explored. The second possibility is to use the advection, dispersion, degradation model, using a groundwater flow model such as Modflow (McDonald & Harbaugh, 1988) or Feflow (Diersch, 2005). If no reactions occur, then the transport in a medium is determined by the advection and the dispersion:

$$\frac{\delta c}{\delta t} = \nabla.(D\nabla c) - \nabla.(\vec{v}c) + Q \qquad \text{(Eq. 6)}$$

where c [g/meter^3] represents the volumetric mass concentration of the contaminant in space and time, ∇ represents the gradient and $\nabla.$ the divergence. Q [g/day] is the external contamination-source rate of injection and D [meter²/day] stands for dispersion. The second term is known as the diffusive flux and the third one the advective flux. The flux velocity vector (v [meter/day]) is calculated from Darcy's law, knowing the hydraulic conductivity (K [m/s]), the porosity (n [/]) and the hydraulic head gradient (∇h [meter])

$$\vec{v} = \frac{-K}{n}\nabla \mathrm{h} \qquad \text{(Eq. 7)}$$

Knowing D, K and n, the migration of AMD towards the saturated flows can be investigated by solving equation 1 with a finite elements model that discretizes a 3D aquifer with movable free surface Feflow ®(Diersch, 2005). The modeled zone (black rectangle in figure 1) was divided into 8 layers of a meter, 26280 mesh nodes and 45296 mesh elements. The south-east and north-west limits of the model were considered to be constant heads, respectively h_{max} and h_{min}. The recharge from the quarry process was modeled as a 500 m^3/day constant flow rate in the basin. The flow velocity was

solved for steady states. The mass concentration (c) was considered to be null at the beginning of the calculation, except in the settling basin, where c at the boundary was constant (Cb [g/meter^3]). The concentrations were solved for each cell and each time using a forward/backward Euler time integration scheme, for a final time of about 1500 days, with adaptive time steps w.r.t. the Peclet and the Courant number (Noorishad et al. 1992).

The basin was simulated as 4000 cells with a 1 m/s hydraulic conductivity and a porosity of about 1. The number of cells filled with water or with the clogged layer changes depending on the various tests described in the following section.

The clogged layer overlay was considered as a low (10^{-8} m/s) hydraulic conductivity layer. Its thickness and its spatial distribution in the basin were determined with the bathymetry measurements. To compare observations and calculations, the calculated water transfer rate (ϕ_c) was defined as follows:

$$\emptyset c = \frac{Qi}{A\,\Delta h} \qquad \text{(Eq. 8)}$$

where Q_i and Δh come from the numerical results.

The mass flux of AMD (F_{AMD} [g/day]) towards the ground water was defined as

$$F_{AMD} = Q_i C_b \qquad \text{(Eq. 9)}$$

where C_b is the mass concentration observed in the basin by Touzé et al. (2014)

2.4. Aquifer properties

The hydraulic conductivity was deduced from aquifer transitivity assuming an aquifer thickness of about 1.5 m. The transmissivity of the aquifer was estimated by a pumping test. A rate of 1m^3/h was pumped during 20h in the PZC well. The drawdown was observed in PZC and PZ2. Transmissivity and storage coefficients were estimated from the analytical solution of Hantush and Jacob (1955).

The dispersivity was estimated from a dye tracer test during the pumping test. 100g of fluorescein was injected in the PZB well, and the recovery curve was observed in the PZC well. Dispersive properties of the aquifer were estimated from an analytical solution for radial converging flow and brief injection with the software TRAC (Gutierrez et al. 2013).

The proposed transport model and the estimation of mass flux towards groundwaters were conducted under the assumption of a non-reactive aquifer. The values obtained are considered to be maxima.

2.4.1 Model validation

The groundwater flows were calibrated using steady state conditions for 3 hydrological conditions.

(1) The June 2011 period is a base flow period before the use of basin B1. The boundary conditions are Qex=0, h_{max} = 110.9m, and hmin =108.2m. (2) The July 2012 period is a base flow period with the use of the basin. Q_{ex}=500m^3/day, h_{max} = 111.2m, and h_{min} =108.2m. (3) The September 2012 period is a high flow period with the use of the basin. Q_{ex}=500m^3/day, h_{max} = 111.3m, and h_{min} =108m. For the 3 runs, only these boundary conditions change. The calculation was validated using a comparison between observed and calculated water heads in the B1 and B2 basins and in the 3 observation wells.

The transport of AMD was validated using the observed concentrations presented in Touzé et al. (2014). A concentration of 0.01 - 0.02 µg/L was measured in June 2013 in the PZ1 and PZ2 wells while it was not observed before.

2.4.2 Parametric tests

The question was to assess whether the transfer rate changed with the increasing size of the settling layer that clogs the interface between the surface waters and the groundwaters. The bathymetry

results and the observed transfer rate (section 3.2) provided field data for comparison with the model results.

The calculated transfer rate (ϕ_c) was estimated for five configurations of the clogged layer. Five runs were done, from an unclogged (0%) to a fully clogged (100%) settling basin. Figure 2 shows an enlargement of the modeled basin 1 (black line) with the mesh used for calculation. Yellow surfaces represent cells with a low hydraulic conductivity value, considered as a clogged zone. The percentage of clogged zone increases from scenario 1 to 5.

In a second step, the calculated transfer rate versus the clogged surface was estimated for a 10^{-2}, 10^{-3} and 10^{-4} m/s aquifer hydraulic conductivity.

3. Results

3.1. Geometric characterization and hydraulic heads

The water elevations observed at the monitoring points are presented in Figure 3. This figure shows seasonal variations of heads in the basin and the groundwaters. In September 2011, the commissioning of Basin 1 created an increase in the basin hydraulic head. If this is compared with the PZ1 water head, a hydraulic gradient inversion can be observed between the basin and the groundwater. The basin, which was at equilibrium with the groundwater, is now higher because of the injected discharge from the quarry activity (Figure 3). The B1 water table shows daily fluctuations, correlated with the discharge in basin B1, highlighted in the figure by a zoom on the April 2012 fluctuations. Water elevation increased during quarry activity, and decreased during closure periods. These daily fluctuations were used to calculate the observed transfer rate.

3.2. Thickness of the clogged layer and observed transfer rate

The volume of settled fine particles was estimated from the four bathymetries of basin B1 (Table 1). In November 2011, 1310 m^3 covered the bottom of the basin. These deposits cover 2850m^2,

representing an increase of about 15% of the basin surface. The volumes and the surface covered with fine particle deposits increased with time.

According to equation 5 and to the water balance of the basin, for the time period where Q_{ex} =0, a decrease of ΔS was observed, making it possible to estimate a transfer rate over time (Fig.4). From 2011 to 2013, the transfer rate was constant, close to 0.02 1/day. The error range was estimated with the error range of the initial parameters. A 20% uncertainty on the evapotranspiration calculation (ETR) gives a 0.001 1/day error range on the transfer rate. A 2mm/day uncertainty on the precipitation (RR) gives a 0.05 1/day error range on the transfer rate calculation. These are the most significant error factors. Thus the observed changes are below the error range of the method and no significant change in transfer rate with time can be observed.

3.3. Aquifer properties

To estimate the aquifer properties, a pumping test was performed. Figure 5a presents the water table drawdowns and the return to equilibrium observed in the PZB well, due to the $1m^3/h$ pumping rate during 0.33 day. The continuous line corresponds to the Hantush and Jacob (1955) model, fitted with observed data, suggesting a transmissivity of about 5 10^{-4} m^2/s and a storage coefficient of about 0.3.

To estimate the dispersive properties, the aquifer was pumped during 0.8 day. Figure 5b presents the tracer breakthrough curve, observed in the PZC well. For technical reasons, the pump was stopped before the end of the test period. The dye tracer was injected at t=0 in the PZB well. The time of first arrival of the tracer was 0.57 days after the injection. An analytical solution of the advection dispersion model (red line) suggests, for a porosity of 0.3, a 1.2 meter longitudinal dispersivity. For a 10 meter scale, these values are consistent with the review by Gelhar et al. 1992.

3.4. ADR model

For each cell, the transport model described in section 3.3 above needs to be further implemented with hydraulic conductivity, porosity and longitudinal dispersivity values. Table 2 summarizes the values applied for the aquifer, the clogged and the basin layers. The values chosen for the clogged layers and the basin are very different in order to simulate surface water and a very low flow layer.

From these properties and with the boundary conditions described above, the model calculates the water flow and the concentration migration in the aquifer. The calculated water heads evidence that the basin is connected with the aquifer. The basin recharges the aquifer. According to Touzé et al. (2014), the concentration in the basin (Cb) is fixed at about 0.2 µg/L. The extent of the plume 700 days after the commissioning of the basin reaches piezometer 2.

3.4.1 Validation

The first validation step was to compare the observed and calculated water heads. A steady state model was selected, but the model was compared with different configurations of the ground water (low or high water) and different configurations of the quarry activity (open or closed). The differences between observed and modeled water heads are below a 0.2% error range. Thus the model gives a correct description of different conditions of the system. The assumption of a steady state to describe the flows thus seems acceptable.

The second step was to validate the model with AMD concentration data. Only a few observation data were available. To validate the calculation, figure 6 shows the breakthrough curves in the PZ1 and PZ2 wells.

The observations show that the first molecules of AMD arrived in the observation wells more than one year after commissioning of the basin. The calculation explains the null concentrations observed during the first year and the increase in concentration in PZ1 and PZ2 after the first year. This is consistent with the PZ2 breakthrough curve that increased two years after the beginning of the

calculation to reach a stationary value close to the lake concentration. The observed concentrations in PZ1 are in the same range as the modeled concentration. The calculated first arrivals in PZ1 occur earlier than the observed ones, suggesting that dispersion processes are over-estimated. Results suggest an advective dominated process in PZ2, with after 4 years, 100% of the water sampled in PZ2 coming from basin 1. It is important to underline that the configuration of the basin enables a low dilution process and that, after four years of advection, the concentrations of groundwater downstream of the basin stabilize close to the basin concentration itself.

3.4.2 Clogged layer and exchanged water

The key parameter that describes the flux toward the aquifer is the water transfer rate. Figure 7 shows the change in the transfer rate versus the percentage of the surface covered by the clogged layer. When the clogged layer spreads out, the transfer rate remains in the same order of magnitude until the area covered reaches 80%. Even if the spreading of the clogged layer involves a decrease in the bottom interface hydraulic conductivity, the stability of the transfer rate can be explained by the observed increase in the basin water level, thus leading to a higher surface transfer rate through the non-clogged surface. Similar results were found by Bru (2014), who showed that the most important contribution to the total transfer rate is by seepage through the bottom surface, which could explain the drastic decrease in the transfer rate when the clogged layer covered more than 80% of the surface. Moreover, it was shown that the fines particles contained in the process water of this case study exhibit very low permeability when just settled and they also have very poor consolidation properties, leading to only a few changes in the permeability of the clogged layer over time. The tests performed show that during the early stage of clogging (surface <80%) the transfer rate is controlled by the hydraulic conductivity of the aquifer. Then for a basin with an advanced stage of clogging, the transfer rate is controlled by the hydraulic conductivity of the clogged layer. The transition is fast, when 90% of the basin is clogged (Fig. 7).

These model results were validated by field observations of the transfer rate (ϕc, blue points in figure 8) plotted versus the percentage of the surface clogged in the basin. The observations confirm a hydraulic conductivity of the aquifer of about 2.10^{-4} m/s. The observed transfer rate remains in the same order of magnitude with the increase in clogging, for a clogging below 50%, which is consistent with the model results.

4. Discussion: seepage of AMD toward the groundwater

In the early stage of the basin, when the clogged layer does not cover the whole surface, the flux remains in the same order of magnitude, controlled by the aquifer properties and the concentration observed in the basin Cb. According to equation 9, or an average basin concentration of about 0.2 µg/L, the AMD flux is estimated to be about 10 g/year. The errors on Cb, K and D estimations suggested that the error range is about ± 5g/year. Compared to the calculation by Touzé et al. (2014), showing that 1.5 kg/year are released in the process, these results suggest that 6 % leaks towards the groundwaters. This value does not take into account the reactivity of AMD in groundwater. In fact, water takes two years to reach PZ2. At this point, the concentrations observed in the groundwater show the same order of magnitude as the calculated concentration using only dilution processes. This suggests that the underground reactivity is low, compared to the reactivity observed in the basin by Touzé et al. (2014).

Touzé et al. (2014) show that AMD is located in the pore waters of the sediments that constitute the clogged layer. The groundwater model suggests a very low water flow in this layer. AMD in clogged layers is stored. In the final stage of the basin, the flux though this layer is controlled by the hydraulic head in the basin. The model suggests a 10^{-8} m/s water flow velocity. According to the observed concentration of about 0.4 µg/L measured in the pore water of the sediments (Touzé et al. 2014), the flux from the clogged layer towards groundwater is estimated to be less than 0.02 g/year without reactivity, in the hydraulic conditions of basin 1 and without artificial recharge.

5. Conclusion

The leakage of AMD, used for flocculation in a settling basin, towards the groundwaters was estimated using a groundwater transport model. The interactions between the surface and the groundwaters were conceptualized using a transfer rate to describe the clogged properties of the interface. The change in the transfer rate as a function of the spread of the clogged layer in the settling basins was characterized with respect to time. It is shown that the water and the acrylamide transfer rate are not controlled by the spreading of the clogged layer until this layer fully covers the interface. When the clogged layer spreads out, the transfer rate remains in the same order of magnitude until the area covered reaches 80%. The main flux takes place through bank seepage. In these early stage conditions of a working basin, the transfer rate is controlled by the hydraulic conductivity of the aquifer. The acrylamide flux towards groundwater remains in the same order of magnitude at close to 10g/year (± 5). In the final stage, the fluxes through the sediments from the settling are controlled by the properties of the clogged sediments. The low flow suggests a low mass flux of less than 0.02 g/year.

This comparison between observed and calculated AMD in groundwater indicates that the reactivity of acrylamide is low compared to dilution processes. The monitoring of observation wells, downstream of the basin, needs to be continued to improve our understanding of the chemical behavior of emergent pollutants in aquifers.

ACKNOWLEDGMENTS: This work was funded by the ANR CES project 1443 AquaPOL, Contaminants, Ecosystèmes, Santé 2010. The authors thank the students Lucie MONNIN and Steeven TESSIER from the Geosciences Master's course at Orléans University for their help during the pumping and tracer tests, the Polytech'Orléans Engineering students Jennifer DEROO and Robin VENAT for their

contribution to developing the model and Dr. Elizabeth ROWLEY-JOLIVET for improving the English language.

REFERENCES

Binet S., Mudry J., Bertrand C., Guglielmi Y., Cova R., (2006).Estimation of quantitative descriptors of northeastern Mediterranean karst behavior: multiparametric study and local validation of the Siou - Blanc massif (Toulon, France) *Hydrogeology Journal* (14) 1107-1121

Binet S, Mudry J, Scavia C, Campus S, Bertrand C, Guglielmi Y (2007) In situ characterization of flows in a fractured unstable slope. *Geomorphology* 86 (1), 193-203

Binet S, Gogo S, Laggoun-Défarge F (2013) A water-table dependent reservoir model to investigate the effect of drought and vascular plant invasion on peatland hydrology. *Journal of Hydrology* 499, 132-139

Brown L, Rhead M (1979): Liquid-chromatographic determination of acrylamide monomer in natural and polluted aqueous environments. *Analyst* 104, 391-399

Bru, K. (2014) Amélioration de la compréhension du fonctionnement d'un bassin de décantation, élément essentiel de la gestion des ressources en eau utilisées par l'industrie extractive des granulats Mines & Carrières (2014) 189-19.

Chu S, Metcalfe CD (2007): Analysis of acrylamide in water using a coevaporation preparative step and isotope dilution liquid chromatography tandem mass spectrometry. Analytical Chemistry 79, 5093-5096

Croll BT, Arkell GM, Hodge RPJ (1974): Residues of acrylamide in water. Water Research 8, 989-993

Dechesne M., Barraud S., Bardin J.-P. (2004) Indicators for hydraulic and pollution retention assessment of stormwater infiltration basins Journal of Environmental Management 71 371–380

Diersch H.J. (2005). Feflow Reference manual Berlin, Germany: WASY GmbH

Gelhar, LW., Welty C., & Rehfeldt K.R. (1992). A critical review of data on field-Scale Dispersion in Aquifers. *Water resources research* (28) 1955-1974.

Guezennec A.G. et al. (2014) Degradation and transfer of polyacrylamide based flocculants in the aquatic environment: a review. *Environmental Science and Pollution Research* (this issue)

Gutierrez A., Klinka T., Thiéry D., Buscarlet E., Binet S., Jozja N., Défarge C., Leclerc B., Fecamp C., Ahumada Y., Elsass J. (2013). TRAC, a collaborative computer tool for tracer-test interpretation. *European Physical Journal* 50 (3002)

Hantush, M. S.; Jacob, C. E. (1955) Non-steady radial flow in an infinite leaky aquifer. Transactions, American Geophysical Union, (36) 95-100

Kalbus E., Schmidt C., Molson J. W. Reinstorf F. and M. Schirmer (2009) Influence of aquifer and streambed heterogeneity on the distribution of groundwater discharge Hydrol. Earth Syst. Sci., 13, 69–77

McDonald MG, Harbaugh AW (1988) MODFLOW, Packages reference manual, Waterloo Hydrogeologic, Waterloo, Canada

Mnif I, Hurel C, Guezennec AG, Marmier N (2014) Interaction of polyacrylamide flocculants and acrylamide with clays, soil and sediments. International Conference on Interfaces against Pollution. May 2014, De Harmonie, Leeuwarden, Netherlands

Muellegger C., Weilhartner A. , Battin T. J. b, Hofmann T. (2013) Positive and negative impacts of five Austrian gravel pit lakes on groundwater quality. Science of the Total Environment 443 (2013) 14–23

Noorishad J., Tsang C. F., Perrochet P., Musy A. (1992). A Perspective on the Numerical Solution of Convection-Dominated Transport Problems: A Price to Pay for the Easy Way Out. *Water Resources Research* (28) 551-561

Packman A.I. and Mackay J.S. (2003) Interplay of stream-subsurface exchange, clay particle deposition and streambed evolution *Water Resources Research* 39, 1097

Rosenberry D.O., Pitlick J. (2009) Effects of sediment transport and seepage direction on hydraulic properties at the sediment–water interface of hyporheic settings *Journal of Hydrology* (373) 377–391

Schubert J. (2002) Hydraulic aspects of riverbank filtration—field studies. *Journal of Hydrology* (266) 145–161

Siriwardene N.R. , Deletic A., Fletcher T.D. (2007)Clogging of stormwater gravel infiltration systems and filters: Insights from a laboratory study Water research (41) 1433 – 1440

Solution, G. N. S. S. (2007). GNSS Solution Software. Version 3.00. 07, Magellan Navigation Company Copyright.

Sophocleous M. (2002) Interaction between groundwater and surface water: state of science. *Hydrogeology Journal* 10, 52-67

Stuart M., Lapworth D., Crane E., Hart A. (2012). Review of risk from potential emerging contaminants in UK groundwater. *Science of the Total Environment* (416) 1–21

Touzé S., Guerin V., Togola A., A.G., Binet S., & Adam Y. (2014) Dissemination of acrylamide monomer from polyacrylamide based flocculant use - sand and gravel quarry case study. *Environmental Science and Pollution Research* (this issue)

FIGURES:

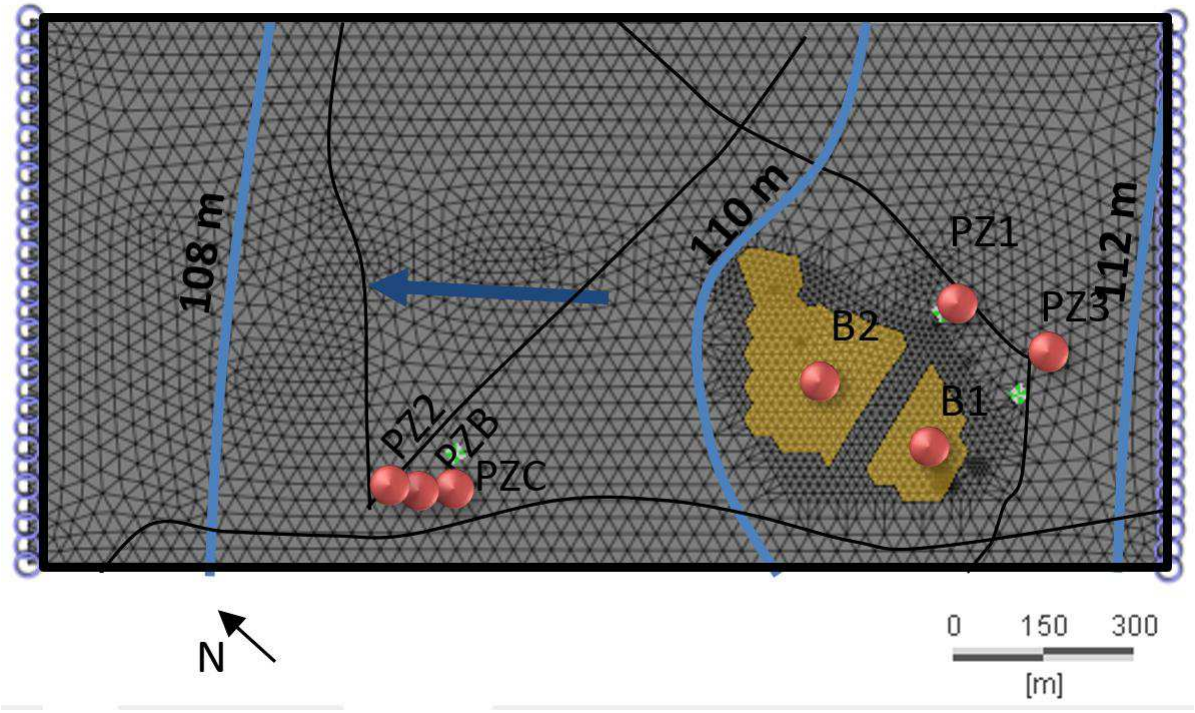

Fig.1: Observation wells (circles) and February 2012 water-head (blue lines) around the quarry basins (yellow surfaces) B1 and B2. Black lines are roads. The black rectangle is the study area boundary for the groundwater model. Grey nodes are the mesh of the hydrodynamic model and blue circle are the constant head (boundary conditions).

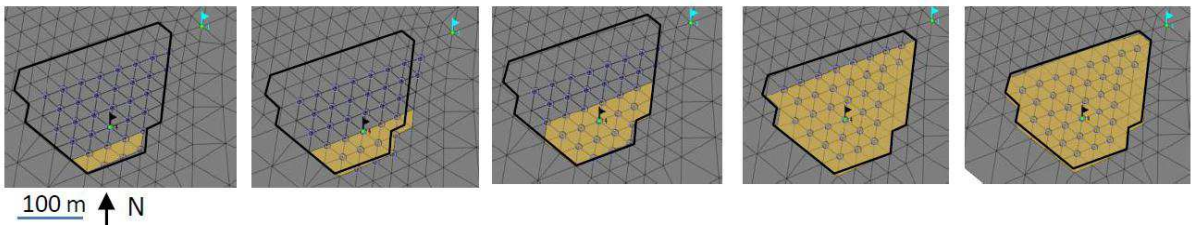

Fig.2: Parametric tests: Map of the scenario of the spreading of the clogged layer (yellow surface) in the basin (black line) used for calculation of the water transfer rate.

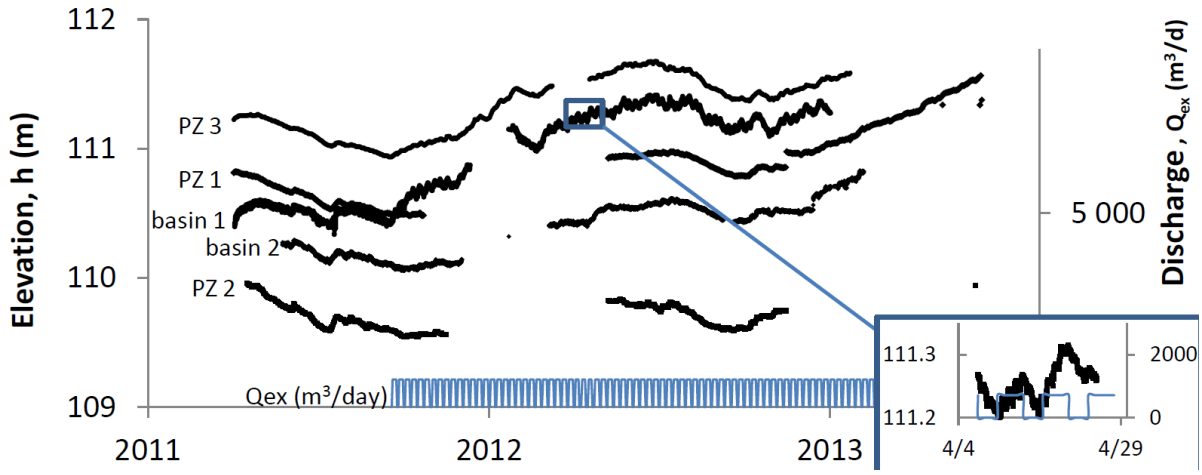

Fig. 3: Hydraulic heads with time in the 2 basins and in the observation wells. Injection discharge in the basin (right axis). The small square on the right is an enlargement of the hydraulic head and of the injection discharge in basin 1 for April 2012.

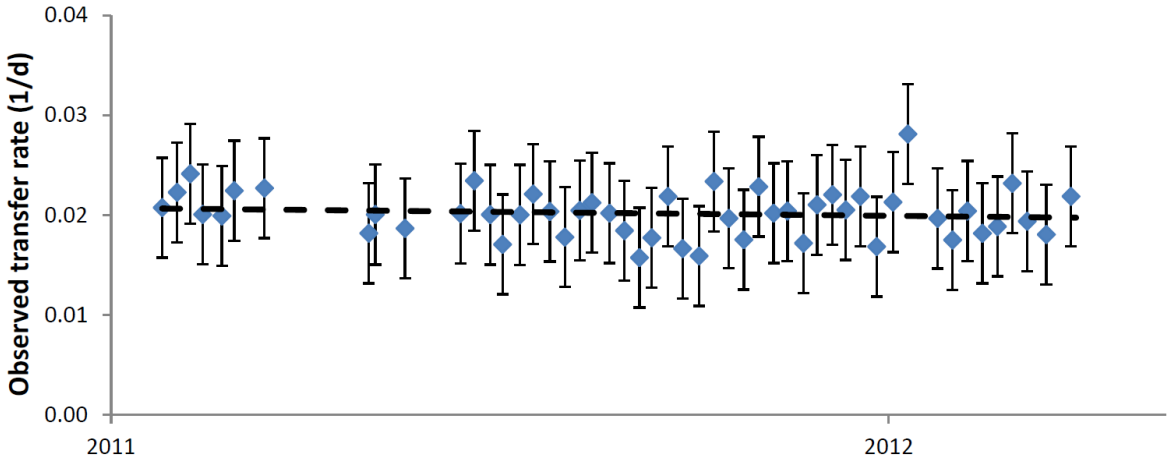

Fig. 4: Observed transfer rate change with time. Given the error ranges, no change can be seen.

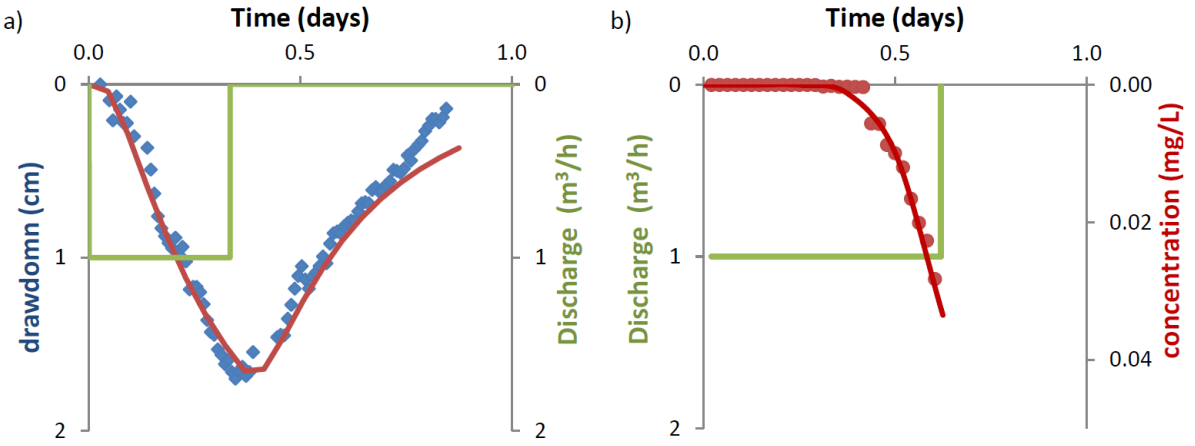

Fig. 5: Pumping test results, a/ drawdown observed and calculated in PZB. b/ concentration breakthrough curve observed and calculated during the pumping test in PZC.

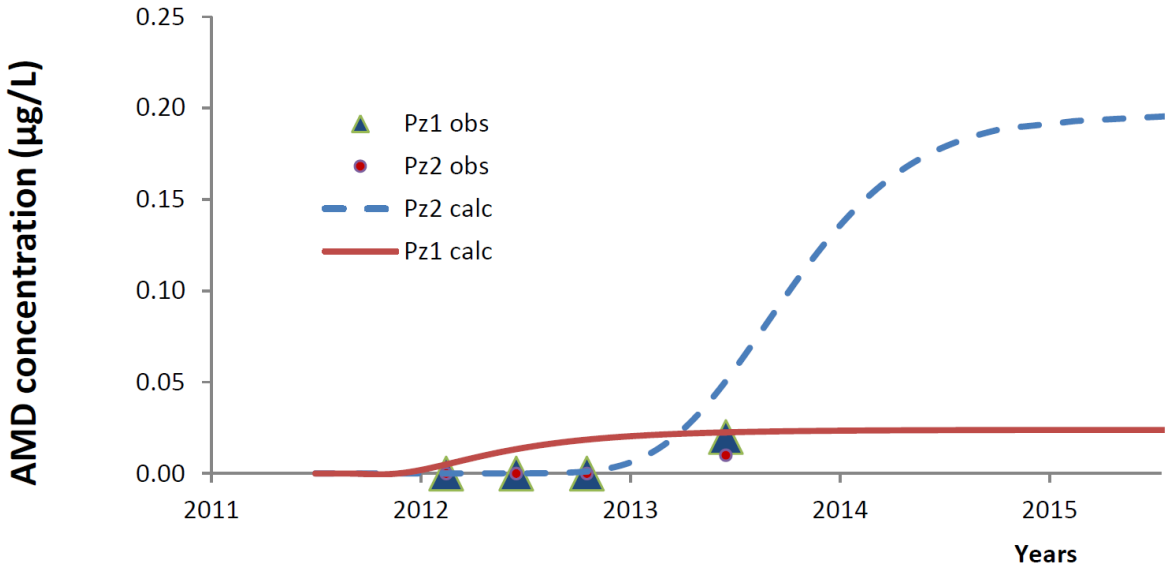

Fig.6: Observed and calculated concentrations versus time of AMD in groundwaters, in the PZ2 (blue) and PZ1 (red) wells. Transient Calculation was applied for transport with steady state hydraulic conditions.

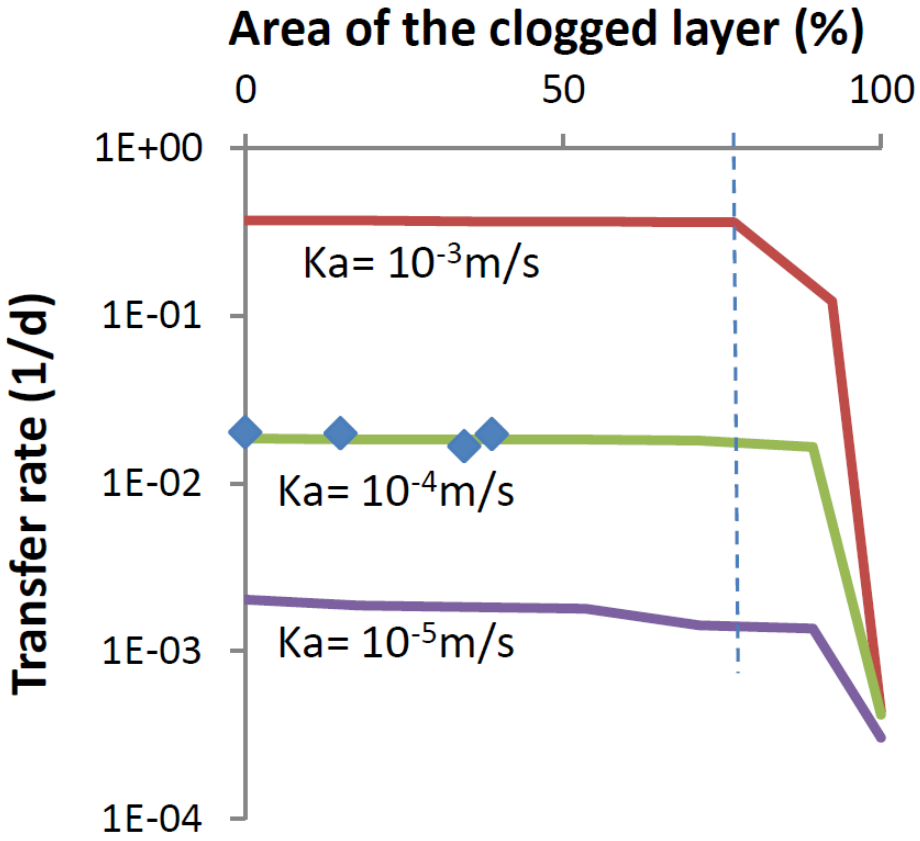

Fig. 7: Observed (blue points) and calculated (line) water transfer rate versus the percentage of area covered by the clogged layer. Calculated values are presented for 10^{-2}, 10^{-3} and 10^{-4} m/s aquifer hydraulic conductivity.

TABLES:

Obs.	13/05/2011	17/11/2011	20/06/2012	16/10/2012
Volume (m^3)		1310	5895	10844
Error (m^3)		142	324	542
Surface (m^2)	0	2850	6554	7380
Surface (%)	0	15	34	39
Φ (1/day)	0.02	0.02	0.02	0.02

Table 1: Volumes and surfaces of the clogged layer with time

	Aquifer	Clogged layer	Basin
K (m/s)	2.E-04	1.E-08	1
ϕ (%)	0.3	0.4	1
D (m)	1.2	1.2	1.2

Table 2: Hydraulic properties of the groundwater transport model.